Available online at www.sciencedirect.com
ScienceDirect
Journal of the European Ceramic Society 27 (2007) 13–18
www.elsevier.com/locate/jeurceramsoc

Temperature dependence of mechanical properties of aluminum titanate ceramics

Chun-Hong Chen *, Hideo Awaji

Department of Materials Science and Engineering, Nagoya Institute of Technology, Gokiso-cho, Showa-ku, Nagoya 466 8555, Japan

Received 29 November 2005; received in revised form 31 March 2006; accepted 14 April 2006
Available online 30 June 2006

Abstract

Aluminum titanate (Al_2TiO_5: AT) is a synthetic ceramic material of potential interest for many structural applications. A critical feature, which greatly limits the mechanical properties of polycrystalline AT, is the considerable intergranular microcracking, which occurs due to the large thermal anisotropy of individual grains during cooling after sintering. This study discusses the temperature dependence of mechanical properties, and presents observations on the microstructure morphology. Both the fracture strength and fracture toughness increased considerably with increasing temperature. The critical frontal process zone (FPZ) size was estimated from the mechanical properties. A decrease in FPZ size was observed with increasing temperature in the first thermal treatment. These phenomena were explained on the basis of the stress redistribution and unique microscopic feature on the fracture surface of AT ceramics. The experimental results revealed that further thermal treatment increased the fracture strength and reduced the fracture toughness, while it had almost no effect on the FPZ size.

Keywords: Al_2TiO_5; Mechanical properties; Fracture; Frontal process zone

1. Introduction

Aluminum titanate ceramics (Al_2TiO_5: AT) are synthetic materials of potential interest for many structural applications owing to their high melting point, low thermal conductivity and excellent thermal shock resistance. Recently, AT ceramics have been used as refractories in aluminum alloy casting systems because they have superior thermal shock resistance and better non-wettability compared to molten aluminum alloys.[1] However, the mechanical properties of polycrystalline AT are greatly limited by grain-boundary microcracking that occurs as a result of the large thermal anisotropy of individual grains during cooling after sintering. At RT, the thermal expansion coefficients of AT ceramics along the three crystalline axes are $\alpha_a = 9.8 \times 10^{-6}\,K^{-1}$, $\alpha_b = 20.6 \times 10^{-6}\,K^{-1}$, $\alpha_c = -1.4 \times 10^{-6}\,K^{-1}$.[2] Grain-boundary microcracking due to the large thermal expansion anisotropy in noncubic polycrystalline ceramics including AT ceramics has been studied extensively.[3–7] The occurrence of microcracking is influenced by the microstructure. The cyclic and static fatigue of AT ceramics was investigated in Al alloy casting systems and the fatigue life was linked to the morphological change of the microcracks.[1,8] The mechanical properties of AT ceramics strongly depend on the microstructure, which in turn is directly related to the degree of microcracking and the stress redistribution in the matrix. The morphology of microcracks in AT ceramics shows a remarkable temperature dependence. As the temperature increases up to the actual casting temperature of 702 °C, the microcracks at the grain boundaries close up, and the AT grains are bonded together by the glassy phase added as sintering aid.[1]

In the present study, the temperature dependence of the fracture strength, fracture toughness and critical frontal process zone size were investigated at actual casting temperatures (from RT to 702 °C). Furthermore, mechanical properties of AT ceramics were examined in relation to the repeated thermal treatment and the microstructure.

2. Experimental procedure

AT ceramics (TM-20, Marusu Glaze Co. Ltd.) were sintered at 1582 °C in the presence of gairome clay. ICP analysis shows

* Corresponding author. Tel.: +81 52 735 5276; fax: +81 52 735 5276.
E-mail address: chunhongqiang@hotmail.com (C.-H. Chen).

0955-2219/$ – see front matter © 2006 Elsevier Ltd. All rights reserved.
doi:10.1016/j.jeurceramsoc.2006.04.182

crystalline components after sintering as Al_2O_3: 52.82, TiO_2: 38.47, SiO_2: 6.31, Fe_2O_3: 1.91, Nb_2O_5: 0.16, K_2O: 0.17, CaO: 0.09 and MgO: 0.06. Mechanical testing was performed using 3 mm × 4 mm × 20 mm rectangular specimens. To reduce the risk of sample failure initiating from an edge, samples were chamfered at 45° using a 10-μm polishing wheel. Four samples of each kind were loaded to failure using a universal test machine (Instron 5581, USA) for fracture strength and toughness measurement. The Instron crosshead speed was 0.5 mm/min, and the span was 16 mm. All mechanical tests were performed at the temperature of the thermal treatment in the mounted furnace. Fracture strengths of longitudinally polished samples were determined by three-point bending. Fracture toughness was measured using the single edge V-notched beam (SEVNB) technique.[9–11] The specimen was notched at the center of its 20 × 4 surface. The depth and radius of curvature of the V-notch of the specimens were 1500 μm and less than 20 μm, respectively.

All the experimental data was obtained from RT to 702 °C. The specimens were heated and quenched at a rate of 575 K/h to the goal temperature and held for 60 min. The first cycle of the thermal treatment was defined as the heating period from RT to the goal temperature. The term second cycle will refer to the subsequent cycle in which the specimen was first quenched to RT and then brought back up to the desired temperature.

The morphological change of the specimens that underwent thermal treatment was observed by SEM (JEOL, JSM-5200). The composition change of the cross-section was examined by X-ray diffractometry.

3. Results and discussion

3.1. Microstructural observation

The SEM micrograph of the polished surface of a specimen is shown in Fig. 1. The gray areas are the AT grains with an average length of about 13 μm, and the dark areas are the pores distributed uniformly throughout the matrix.

Fig. 2 shows SEM micrographs of fracture surfaces of the specimens at RT: (a) without thermal treatment, (b) after the first thermal treatment, and (c) after the second thermal treatment.

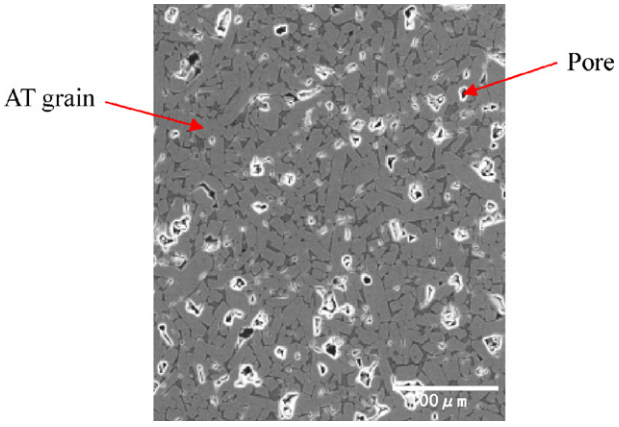

Fig. 1. SEM micrograph of the polished surface of the specimen.

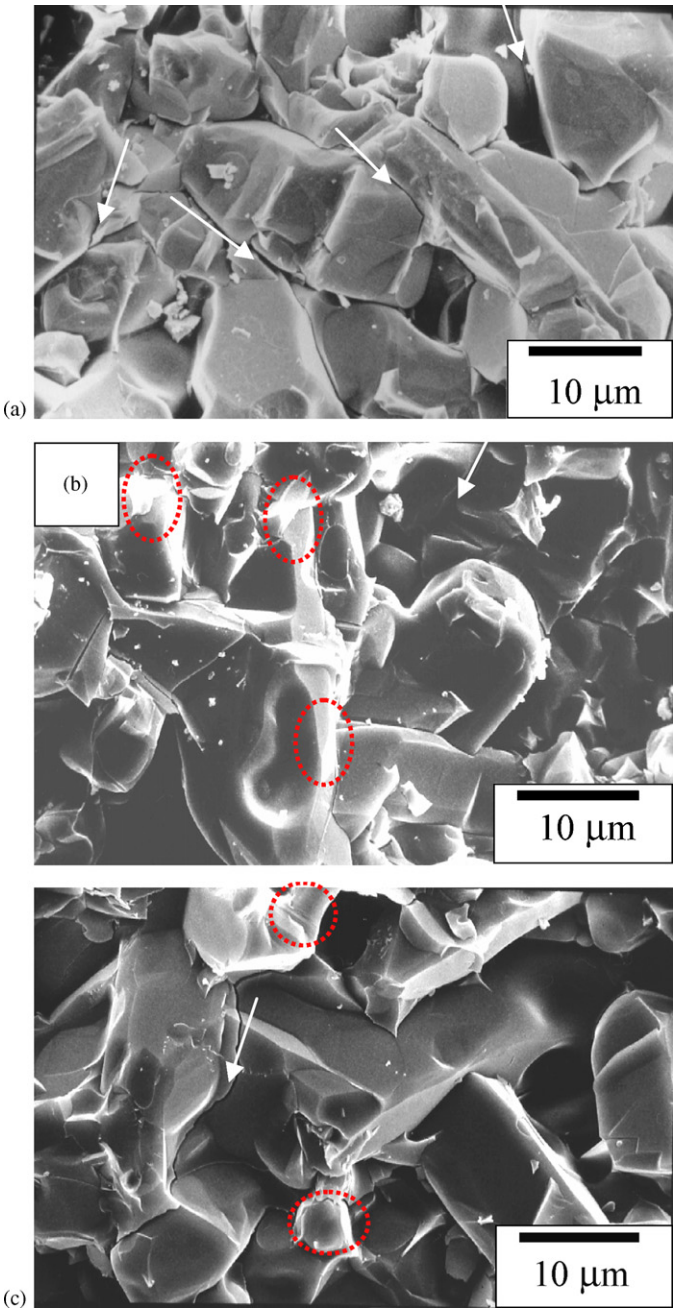

Fig. 2. SEM micrographs of the fracture surface at RT: (a) without heat-treatment, (b) after the first cycle and (c) after the second cycle.

The white arrows indicate the microcracks, and the dotted red circles show the glassy agglomerates. There are many microcracks along the grain boundary in the matrix at RT as can be seen in Fig. 2(a). The microcracking is believed to be caused by the variation in the thermal expansion coefficient of the AT grains with the crystalline direction, giving rise to boundary stresses. These are often sufficient to initiate small cracks. Stresses generated during cooling of the samples from the sintering temperature can also induce microcracking without leading to ultimate fracture. At high temperature, the microcracks close up and self-heal thanks to the glass phase. The initiation and self-healing of microcracks occur repeatedly as a result of repeated

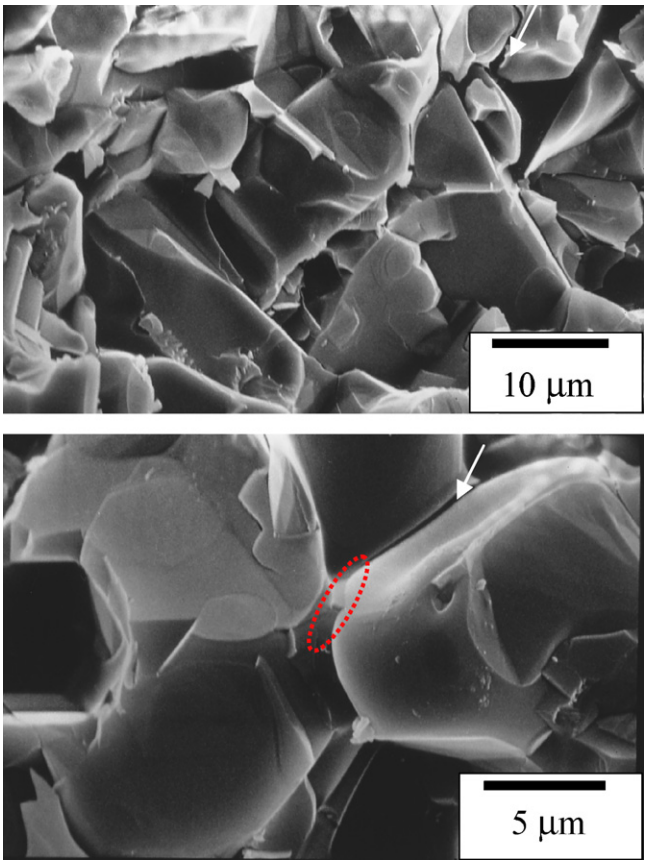

Fig. 3. SEM micrograph of fracture surface at 702 °C after the second cycle.

cooling from 702 °C to RT. Thus, the microcrack density is lower (see Fig. 2(b) and (c)), as compared to the case without thermal treatment. This is because the glass phase separates from the interconnected structure, and a large amount of glass is entrapped in the AT matrix as can be seen in the micrographs.

No large difference in microstructure of the fracture surface is observed at 702 °C after the first and second cycles (see SEM micrographs in Fig. 3). Less intergranular microcracking is observed on the fracture surface at 702 °C compared with that at RT. The triple-junction glass phase withdraws and leads to the formation of the segregated glass phase at the grain boundaries. However, X-ray diffractometry revealed that heat-treatment did not alter the phase composition despite the presence of the color fade-out.

3.2. Physical properties of AT ceramics

Fig. 4 shows the temperature dependence of the elastic modulus and thermal conductivity of AT ceramics from RT to 702 °C. The thermal conductivity and elastic modulus were measured by the laser flash method (JIS R 1611) and bend resonance method (JIS R 1602), respectively. The thermal conductivity gradually decreased with temperature down to 502 °C, owing to the contraction from the negative expansion crystal axis and the microcrack occlusion from the positive expansion crystal axis. An abrupt increase in elastic modulus and thermal conductivity occurred above 502 °C, which suggested that the closed crack

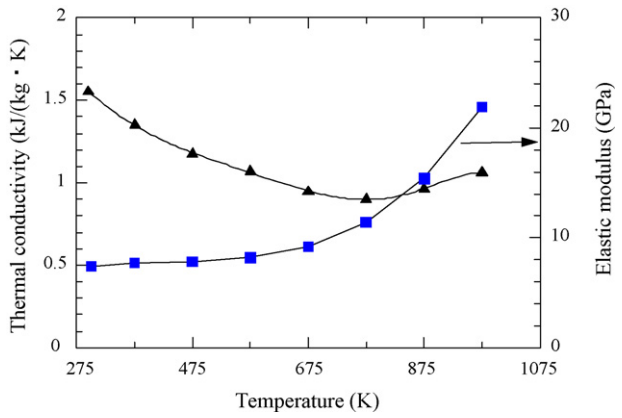

Fig. 4. Temperature dependence of elastic modulus and thermal conductivity in AT ceramics.

surfaces were self-healing and causing bonding of AT grains by the glass phase in the matrix.

A thermal hysteretic behavior was observed in the heating and cooling period in the linear thermal expansion properties of AT ceramics, as shown in Fig. 5. The curves in the figure pertain to TM-20 and TM-19, AT ceramic products by Marusu Glaze Co. ICP analysis shows the difference in the composition of the glass phase between TM-19 and TM-20, especially in SiO_2 content (TM-19: 8.1 mass%, TM-20: 6.31 mass%). This can be explained by accumulated microcracking due to the thermal expansion anisotropy of the individual AT crystals, which gives rise to stresses on a microscopic scale during cooling. These localized internal stresses constitute the driving force for microcracking. Clearly, the difference in the composition of the glass phase has a great effect on the contraction and expansion of AT crystals.

3.3. Temperature dependence of mechanical properties

The fracture strength (σ_B) was estimated using the equation:

$$\sigma_B = \frac{3PS}{2WH^2} \quad (1)$$

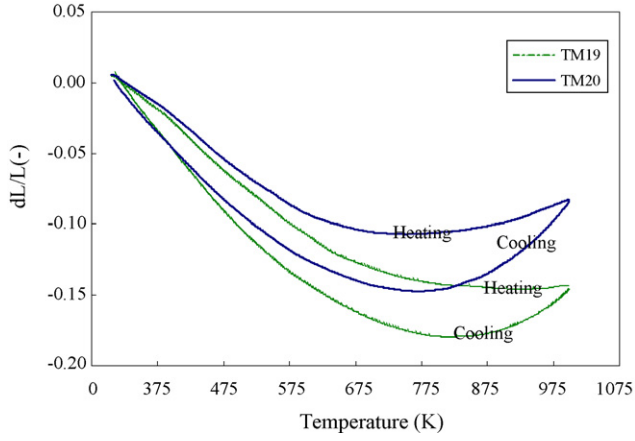

Fig. 5. Linear thermal expansion properties of AT ceramics (TM-20 and TM-19).

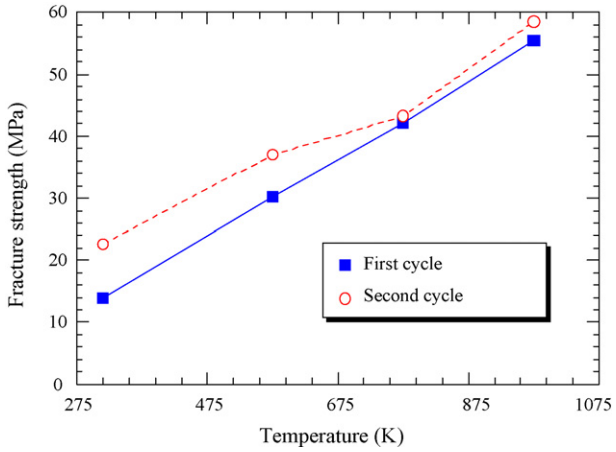

Fig. 6. Temperature dependence of fracture strength in AT ceramics.

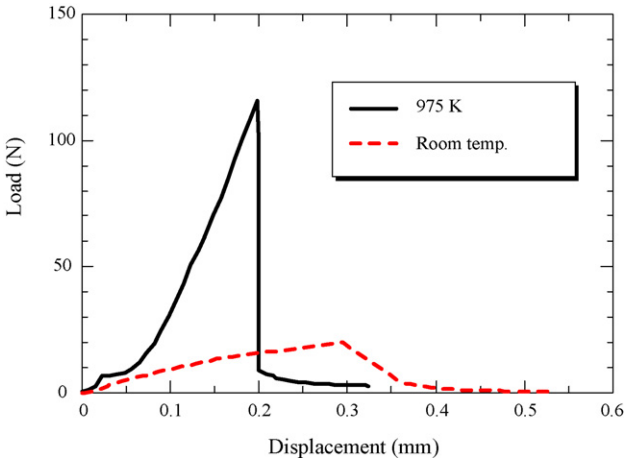

Fig. 7. Load–displacement curves after fracture at RT and 702 °C.

where P is the applied maximum load, S the span length, and W and H are the width and height of the polished specimen, respectively.

The intrinsic fracture toughness (K_{IC}) was evaluated by using the stress intensity factor estimated by Wakai et al.[12]:

$$K_{IC} = Y\sigma_{fc}a^{1/2}, \quad Y = \sum_{i=0}^{4} A_i\lambda^i, \ \lambda = \frac{a}{H},$$

$$A_i = a_i + b_i \ln\left(\frac{S}{H} - c_i\right) \tag{2}$$

$$\sigma_{fc} = \frac{3PS}{2WH^2} \tag{3}$$

where Y represents the shape factor of the test specimen, a the length of the crack, S the span length, P the applied maximum force, and σ_{fc} the critical stress on the tensile surface of the flexure specimen.

Fig. 6 shows the temperature dependence of the fracture strength after the thermal treatment. The experimental results show that the fracture strength of AT ceramics increases with increasing process temperature due to a decrease in the number of microcracks along the AT grain boundaries during bonding of the AT particles via the glass phase at higher temperatures.

The phenomenon can also be explained from the load–displacement curve after fracture shown in Fig. 7. The displacement at maximum load at RT is higher compared to that at high temperature (702 °C) owing to the higher concentration of microcracks at RT. A stable fracture behavior is obtained at RT, where no obvious initial linear elastic region is observed before attainment of the maximum load. This is because the failure under loading occurs only in the glass phase and the cracks propagate along the glass layer around the AT grain boundaries. This is not the case at high temperature, where the unstable fracture behavior is similar to that in dense ceramics.

The fracture strength was further improved by the second cycle of thermal treatment due to the stress redistribution in the AT grains. This is presumably because an intergranular strain is generated upon sintering, when a high concentration of microcracks form in the quenching process due to the hysteresis and anisotropy of the thermal expansion coefficient of AT ceramics.[1] The residual stresses in the grain are released after repeated thermal treatment. However, no large difference in strength or toughness remains after the third cycle, as compared with that after the second cycle. One reason for this is that it is impossible to eliminate residual stresses completely by thermal treatment, and thus, the susceptibility of AT ceramics to thermal effects is lowered. Another factor is thought to be the fact that the glass structure is stabilized during the repeated heat-treatment which helps to avoid variation in properties.[13]

The temperature dependence of fracture toughness after the thermal treatment is shown in Fig. 8. The fracture toughness increased with increasing temperature. After the second thermal treatment, the fracture toughness was reduced compared to the first thermal treatment, except at RT. Clearly, the relationship that exists between fracture toughness and strength to the temperature after the first cycle of heat-treatment is reversed after the second cycle of thermal treatment. This is presumably because different mechanisms of initial phase separation are at play at different temperatures, depending on the past thermal history.

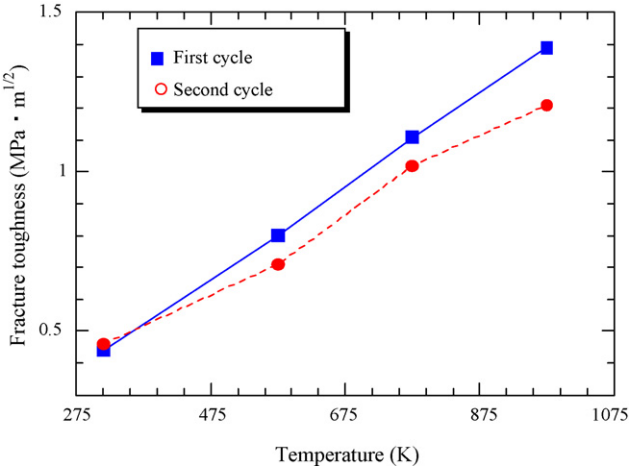

Fig. 8. Temperature dependence of fracture toughness in AT ceramics.

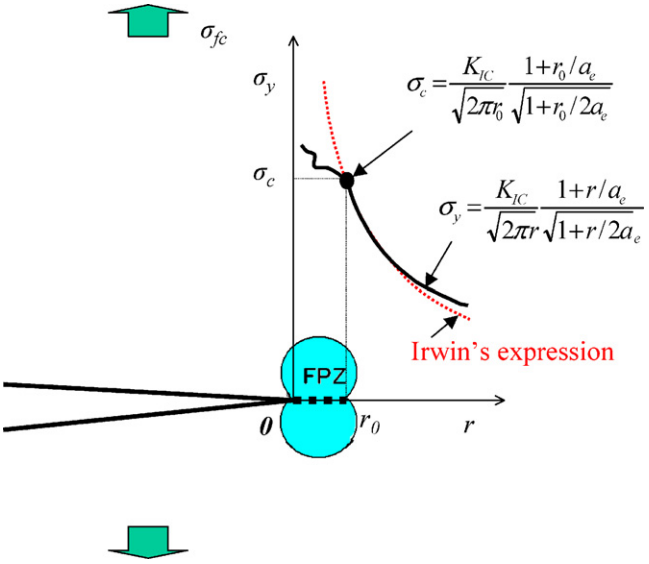

Fig. 9. The frontal process zone around a crack tip.

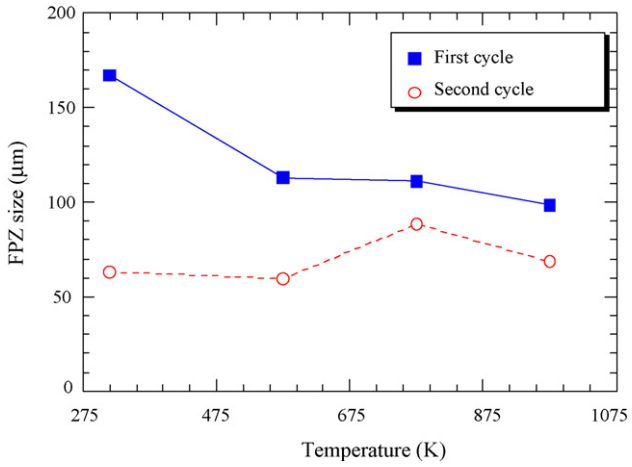

Fig. 10. Temperature dependence of the front process zone size in AT ceramics.

3.4. Temperature dependence of frontal process zone size

Previous reports have proven that the frontal process zone (FPZ) at the crack tip of ceramics is an important factor in assessing the toughening mechanism.[9–12,14,15] Owing to the minuteness and indistinctness of the FPZ size, there are no suitable techniques for estimating the FPZ size, but only an indirect method using the SEVNB technique.[9–11]

The local fracture criterion states that a crack will propagate when the stress at a critical distance from the crack tip reaches a critical value.[11,16] The critical FPZ size is defined in terms of this critical distance, as shown in Fig. 9. Based on the local fracture criterion of linear fracture mechanics, the critical FPZ size (r_0) is given by[11,16]:

$$r_0 = \frac{1}{2\pi}\left(\frac{K_{IC}}{\sigma_C}\right)^2 \cong \frac{1}{2\pi}\left(\frac{K_{IC}}{\sigma_B}\right)^2 \quad (4)$$

where K_{IC}, σ_B, σ_C are the fracture toughness, fracture strength and local fracture stress, respectively.

Fig. 10 shows the effect of heat-treatment on the size of the critical FPZ. The critical FPZ size is 167 μm at RT without heat-treatment. This is 20 times higher compared to that of other dense ceramics, whose critical FPZ size is almost less than 10 μm.[5] After the first cycle of thermal treatment, the critical FPZ size decreases with increasing temperature, down to 100 μm at 702 °C. The residual stress is released at the grain boundary. An intergranular strain is generated after sintering, when many microcracks form in a quenching process due to the hysteresis and anisotropy of the thermal expansion coefficient of AT ceramics.[1] At low temperatures, the domain where the above-mentioned phenomenon is observed is enlarged due to the increased number of microcracks. The intergranular strain is gradually eliminated with the softening of the glass phase in the matrix and the adhesion/recombination of the microcracks at higher temperatures, hence the lower size of the critical FPZ.

However, after two cycles of thermal treatment, the critical FPZ size is reduced to about 65 μm, and almost keeps a constant value, except at the test temperature 502 °C. This is because the degradation in the degree of crack adhesion and the elimination of the intergranular strain do not appreciably change the domain subjected to the stress relief.

4. Summary

Three-point bending tests on AT ceramics were carried out from ambient temperature to 702 °C. The temperature dependence of physical and mechanical properties was examined, and the microstructure was characterized. The sintered samples were subjected to repeated thermal treatment to investigate the change in mechanical properties of AT ceramics. Both the fracture strength and fracture toughness increased considerably with increasing temperature due to the difference in the microcrack morphology. The second thermal treatment improved fracture strength and reduced fracture toughness. No appreciable difference in mechanical properties was observed after the third thermal treatment because of the decrease in the susceptibility of AT ceramics to thermal-history effects. The critical frontal process zone (FPZ) size was found to decrease with increasing temperature in the first heat-treatment and almost no changes occurred upon further heat-treatment.

References

1. Matsudaira, T., Kuzushima, Y., Kitaoka, S., Awaji, H. and Yokoe, D., Temperature dependence of static and cyclic fatigue behavior of Al_2TiO_5 ceramics. *J. Ceram. Soc. Jpn.*, 2004(Supplement 112-1, PacRim5 Special Issue), S327–S332.
2. Morsin, B. and Lynch, R. W., Structure studies on Al_2TiO_5 at room temperature and at 600 °C. *Acta Cryst. B*, 1972, **28**, 1040.
3. Ohya, Y. and Nakagawa, Z., Grain-boundary microcracking due to thermal expansion anisotropy in aluminum titanate ceramics. *J. Am. Ceram. Soc.*, 1987, **70**(8), C184–C186.
4. Dhingra, A. K., Alumina fiber FP. *Philos. Trans. R. Soc. Lond. A*, 1980, **294**, 411–417.
5. Birchall, J. D., Bradbury, J. A. A. and Dinwoodie, J., Alumina fibers: preparation, properties and applications. In *Handbook of Composites, Strong*

Fibers, *Vol 1*, ed. W. Watt and B. V. Perov. Elsevier, Amsterdam, The Netherlands, 1985.
6. Birchall, J. D., The preparation and properties of aolycrystalline aluminum oxide fibers. *Trans. J. Br. Ceram. Soc.*, 1983, **82**, 143–145.
7. Ohya, Y. and Nakagawa, Z., Measurement of crack volume due to thermal expansion anisotropy in aluminum titanate ceramics. *J. Mater. Sci.*, 1996, **31**, 1555–1559.
8. Mathumura, Y., Characterization of Al_2TiO_5 ceramics. Master Thesis. Nagoya Institute of Technology, 2004.
9. Awaji, H. and Sakaida, Y., V-Notch technique for single-edge notched beam and Chevron notch methods. *J. Am. Ceram. Soc.*, 1990, **73**(11), 3522–3523.
10. Awaji, H., Choi, S.-M. and Jayaseelan, D. D., Indirect estimation of critical frontal process zone size using a single-edge V-notched-beam technique. *J. Ceram. Soc. Jpn.*, 2001, **109**, 591–595.
11. Chen, C. H., Awaji, H. and Choi, S. M., Critical frontal process zone size and fracture toughness. *J. Ceram. Soc. Jpn.*, 2004(Supplement 112-1, PacRim5 Special Issue), S418–S422.
12. Wakai, F., Sakaguchi, S. and Matuno, Y., *J. Ceram. Soc. Jpn. (Yogyou-kyokai-shi)*, 1985, **93**, 479–480 [in Japanese].
13. Kingery, W. D., Bowen, H. K. and Uhlmann, D. R., *Introduction to Ceramics* (*2nd ed.*). John Wiley & Sons, Inc., 1975, pp. 816–846.
14. Hoagl, R. G. and Embury, J. D., A treatment of inelastic deformation around a crack tip due to microcracking. *J. Am. Ceram. Soc.*, 1980, **63**, 404–410.
15. Evans, A. G. and Faber, K. T., Toughening of ceramics by circumferential microcracking. *J. Am. Ceram. Soc.*, 1981, **64**, 394–398.
16. Chen, C. H., Fabrication and characterization of dense and porous ceramics-based tubes of functionally gradient materials. Doctor Thesis. Nagoya Institute of Technology, 2005.